Block Copolymers

DOI: 10.1002/anie.201004445

Block Copolymers Comprising π-Conjugated and Liquid Crystalline Subunits: Induction of Macroscopic Nanodomain Orientation**

*Dehui Han, Xia Tong, Yi Zhao, and Yue Zhao**

The tuning of microphase separation and self-organization in block copolymers (BCPs) with π-conjugated subunits (rod–coil or rod–rod) is a promising means to control the microstructure or morphology that may be crucial for the electronic and optoelectronic applications of such BCPs.[1] In the case of BCPs based on poly(3-hexylthiophene) (P3HT),[2–7] which is one of the most important conducting polymers, as regioregular P3HT has a very high melting temperature T_m, a long-range ordered morphology is difficult to obtain, because of the dominant crystallization process that competes with self-assembly.[3] As a consequence, it is even more challenging to obtain nanodomains of P3HT that are preferentially oriented in one direction at a macroscopic scale. The development of a technique for the manipulation of a phase-separated morphology and ordered nanodomains in P3HT-based BCPs is thus of general interest. We report herein a study designed to address this important issue.

We synthesized a P3HT-based copolymer, which, to the best of our knowledge, is the first diblock copolymer composed of regioregular P3HT and a side-chain liquid crystalline polymer (SCLCP) that bears azobenzene mesogens (Table 1). Previously, Yu et al.[8,9] and Morikawa et al.[10,11] showed that the macroscopic orientation of cylindrical nanodomains of PEO or PS could be obtained by orienting azobenzene mesogens either optically[9–11] or along the rubbing direction of a rubbed surface[8] by using BCPs of an azobenzene-containing SCLCP with either poly(ethylene oxide) (PEO) or polystyrene (PS). The fact that crystalline PEO has a low T_m value and PS is amorphous accounts for the ease of orientation of their nanodomains. However, it is challenging to achieve the same effect for P3HT for the reasons mentioned above. The design principle of our BCP is as follows: to induce orientation of azobenzene mesogens by either surface effects or by linearly polarized light,[12] the BCP needs to be thermally annealed in a liquid-crystalline (LC) phase of the SCLCP block, while P3HT should be in the isotropic state ($T > T_m$) to facilitate the microphase separation and allow fluid nanodomains of P3HT to be oriented by an anisotropic environment of oriented mesogens. This prerequisite means that the SCLCP should have a high LC→isotropic phase transition (clearing) temperature. The SCLCP used to construct the BCP with P3HT, namely, poly{4-[4-(6-methacryloyloxyhexyloxy)benzoate]-4′-hexyloxyazobenzene} (PAzoMA), meets the criterion. With an extended mesogenic core that contains three phenyl rings, PAzoMA has a clearing temperature of approximately 240 °C,[13] which is higher than the T_m value of P3HT. With this BCP, we found that surface-induced orientation of mesogens could align striplike nanodomains of P3HT in the same direction. Likewise, photoinduced orientation of mesogens could also result in a certain degree of macroscopic orientation of the nanodomains. This proof-of-principle study thus demonstrates that the use of LC field-induced alignment is a pathway to achieving and manipulating macroscopic orientation of nanodomains of conducting polymers.

Table 1: Chemical structure of the block copolymers and characteristics of the synthesized samples.

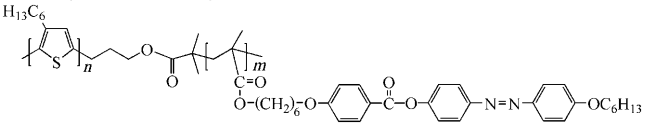

Sample	M_n[a] [g mol^{-1}]	M_n[b] [g mol^{-1}]	PDI[b]	P3HT [wt%]
$P3HT_{26}$-Br	4510	6400	1.12	100
$P3HT_{26}$-*b*-$PAzoMA_{23}$	17990	22650	1.15	25
$P3HT_{26}$-*b*-$PAzoMA_{36}$	25610	27350	1.18	17
$P3HT_{43}$-Br	7330	10150	1.13	100
$P3HT_{43}$-*b*-$PAzoMA_{38}$	29600	32200	1.26	25
$P3HT_{43}$-*b*-$PAzoMA_{120}$	75540	76500	1.32	10

[a] Determined by ^{1}H NMR spectroscopy in $CDCl_3$. [b] Determined by size exclusion chromatography, using polystyrene standards and THF as eluent.

The obtained BCP samples of P3HT-*b*-PAzoMA, that is, two regioregular P3HT macroinitiators and four BCPs of varying compositions, are listed in Table 1. The P3HT macroinitiator was first obtained by using a previously reported method,[14] and was then used to grow the second block of PAzoMA through atom transfer radical polymerization (ATRP). Figure 1 shows examples of characterization results for $P3HT_{43}$-Br and $P3HT_{43}$-*b*-$PAzoMA_{120}$. The size exclusion chromatography (SEC) curves show that the as-obtained BCP contained a small fraction of nonreacted P3HT (Figure 1a), but it could readily be removed by a fractionated

[*] D. Han, X. Tong, Y. Zhao, Prof. Y. Zhao
Département de chimie, Université de Sherbrooke
Sherbrooke, Québec J1K 2R1 (Canada)
Fax: (+1) 819-8218017
E-mail: Yue.Zhao@Usherbrooke.ca
Homepage: http://pages.usherbrooke.ca/yzhao/

[**] We acknowledge financial support from the Natural Sciences and Engineering Research Council of Canada (NSERC) and le Fonds québécois de la recherche sur la nature et les technologies (FQRNT, Québec). Y.Z. is a member of the FQRNT-funded Center for Self-Assembled Chemical Structures. We also thank Mrs. Rodica Neagu-Plesu (Laval University) for help with the X-ray diffraction measurements.

Supporting information for this article (details of block copolymer synthesis and characterization) is available on the WWW under http://dx.doi.org/10.1002/anie.201004445.

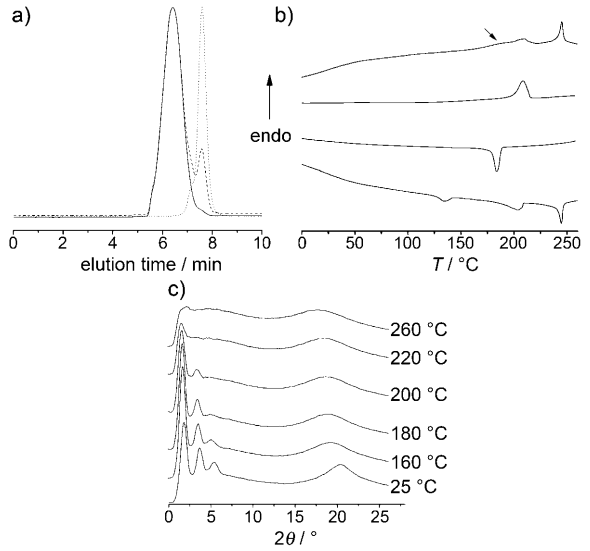

Figure 1. a) Size-exclusion chromatograms of a P3HT macroinitiator (•••••) and $P3HT_{43}$-*b*-$PAzoMA_{120}$ block copolymer before (-----) and after (——) fractionation; b) Differential scanning calorimetry (DSC) curves (heating and cooling scans) of the P3HT macroinitiator (two curves in the center) and the block copolymer (two outer curves); the arrow indicates P3HT crystal melting at ca. 180°C; c) Variable-temperature X-ray diffractograms of the block copolymer.

precipitation, thus giving rise to a BCP sample with a low polydispersity index (PDI) for P3HT-based BCPs. DSC heating and cooling curves confirmed that the PAzoMA block has a clearing temperature higher than the T_m of the P3HT block (Figure 1b). While $P3HT_{43}$-Br exhibits an exothermic peak that indicates a crystallization temperature $T_c \approx 182$ °C on cooling from the isotropic state and a melting endothermic peak at approximately 206 °C on heating, the BCP shows two additional mesophase transitions from the SCLCP block at higher temperatures. On cooling, the first two exothermic peaks at 242 °C and 208 °C correspond to the isotropic→LC1 and LC1→LC2 phase transition respectively, and the peak at approximately 135 °C arises from the crystallization of the P3HT block. On heating, the crystal melting of P3HT occurs at approximately 180 °C (indicated by an arrow in Figure 1b), and is partially overlapped with the endothermic peak of the LC2→LC1 transition, while the clearing (LC1→isotropic) temperature is about 240 °C. These phase transition assignments were confirmed by variable-temperature X-ray diffractograms of $P3HT_{43}$-*b*-$PAzoMA_{120}$ (Figure 1c). The diffraction peak at $2\theta \approx 5.4°$ (*d* spacing: 16.5 Å) at 25 °C arises from crystallized P3HT chains, while the other two peaks at $2\theta \approx 1.8°$ (*d* spacing: 49 Å) and 3.7° (*d* spacing: 24 Å) arise from a smectic phase (LC2) of PAzoMA. Crystalline P3HT melted upon heating to 180 °C, the LC2→LC1 phase transition was completed at 220 °C with PAzoMA in a less ordered nematic phase with smectic ordering (polarized optical microscopy (POM) images in the Supporting Information), while the PAzoMA block was in the isotropic phase at 260 °C. These results confirm that the main feature of our BCP design was successful, that is, the P3HT block crystallizes in the BCP, but has a T_m value lower than the clearing temperature of the SCLCP. It is interesting to note that from Figure 1b, the supercooling of P3HT, defined as T_m-T_c, is larger for the BCP (approximately 45 °C) than for $P3HT_{43}$-Br (approximately 24 °C). This result reflects the increased difficulty of crystallization under the effect of nanodomain confinement and interfacial interactions with PAzoMA. Similar characterization results were obtained with other BCPs (Table 1).

The effect of surface-induced LC orientation on the phase-separated morphology of $P3HT_{43}$-*b*-$PAzoMA_{120}$ was first investigated. A thin BCP film was spin-coated on a glass slide with a rubbed polyimide layer on the surface (LC cell, E.H.C., Japan); after drying, the film was cooled from 260 °C (isotropic phase) to 220 °C within 10 minutes for orientation of the mesogens (with P3HT in the isotropic state and PAzoMA in the LC phase), and was then slowly cooled to room temperature. For comparison, another film was cast on a nonrubbed quartz surface and was subjected to the same thermal treatment (the film thickness was about 30 nm). Figure 2a, b show the AFM phase images of the films over an area of 1 μm × 1 μm, the fast Fourier transform (FFT) of the images (lower left), as well as their polarized UV/Vis spectra (lower right), respectively. In both films, P3HT was well phase-separated from PAzoMA and formed stripelike nanodomains (lighter color) as in other P3HT-based BCPs.[4–5] On the nonrubbed surface (Figure 2a), P3HT nanodomains are randomly oriented on the macroscopic scale, as are the mesogens in PAzoMA, the random orientation of which is indicated by the absence of dichroism of the azobenzene absorption band around 360 nm. By contrast, on the rubbed surface (Figure 2b), the orientation of mesogens along the rubbing direction can be seen from the large dichroic ratio of their absorption band, and P3HT stripelike nanodomains are uniformly aligned in the same direction as the LC orientation. In this case, the enhanced periodicity in the direction perpendicular to the aligned P3HT stripes is also reflected by the FFT pattern. These results show that an oriented SCLCP could align phase-separated, stripelike nanodomains of P3HT in the isotropic phase, and this macroscopic orientation of P3HT nanodoamins remains intact upon crystallization of P3HT when cooling to room temperature. The crystalline packing of P3HT chains in the nanodomains is indicated by the absorption band of the thiophene rings around 520 nm. However, in the oriented film, the small dichroism of the thiophene band implies that P3HT chains inside the aligned stripe-like nanodomains are not preferentially oriented along the rubbing direction. This result is in contrast to the chain orientation observed for a conducting polymer soluble in a small-molecule nematic LC.[15] Without annealing the BCP with P3HT in the isotropic state, a uniform orientation of the stripelike P3HT nanodomains could not be obtained.

Photoinduced orientation of the azobenzene mesogens in a SCLCP like PAzoMA could be accomplished by first exposing a thin film to nonpolarized UV light (360 nm) in order to convert *trans* isomers into *cis* isomers, and by then irradiating the film with linearly polarized visible light (440 nm) to convert the *cis* isomers back into the *trans* form while inducing a molecular orientation of the chromophore

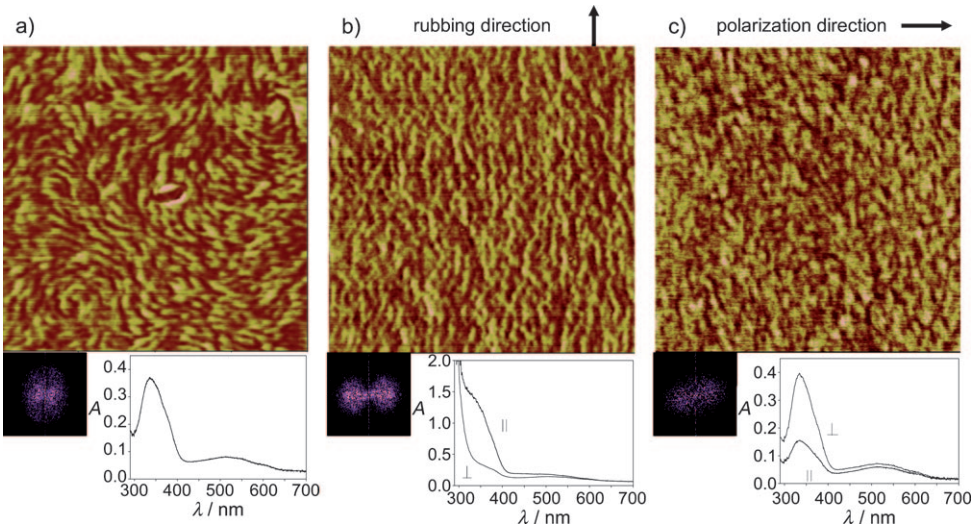

Figure 2. AFM phase images (1 μm × 1 μm), their corresponding fast Fourier transformations, and polarized absorption spectra for thin films of $P3HT_{43}$-*b*-$PAzoMA_{120}$ cast on a) a nonrubbed quartz plate, b) a rubbed glass plate for surface-induced orientation of the mesogens, and c) a nonrubbed quartz plate subjected to irradiation for photoinduced orientation of the mesogens. Absorption spectra were recorded with the beam of the spectrophotometer polarized to be parallel and perpendicular, respectively, to either the surface-rubbing direction (b) or the polarization of the irradiating light (c).

perpendicular to the polarization of visible light.[12] This photoinduced orientation can be enhanced by annealing the film to above the T_g value of the polymer because of a cooperative rearrangement motion of mesogens promoted by polymer chain mobility. However, we found that such a photoinduced and thermally enhanced orientation of azobenzene mesogens decreases at $T > 160\,°C$, which is close to the melting point of crystalline P3HT. Therefore, we had to anneal the BCP film at lower temperatures to preserve the high degree of LC orientation. Given that the crystallization of P3HT may hamper the formation of a long-range ordered morphology,[3] the possibility of using photoinduced orientation to macroscopically align the nanodomains of P3HT was investigated under the following conditions: a film of $P3HT_{43}$-*b*-$PAzoMA_{120}$ was solution-cast on a quartz plate and dried at room temperature. No well-developed microphase separation was observed in AFM in the as-cast film. The film was subjected to irradiation by UV and visible light at 45 °C to induce orientation of the azobenzene mesogens and, after turning off the irradiation, the film was thermally annealed at 120 °C for 1 hour before cooling to room temperature (T_g of PAzoMA in the BCP is about 45 °C). Figure 2c shows the AFM phase image, FFT, and polarized UV/Vis spectra of the film recorded after the optical and thermal treatment. The strong dichroism of the azobenzene absorption band indicates orientation of mesogens in the expected direction, that is, perpendicular to the polarization of the visible light irradiation. The nanodomains of P3HT appear to be less well developed because of their lower annealing temperature. Nevertheless, the alignment of the mesogens along the LC orientation direction is obvious from the phase image and FFT (the apparent tilt of oriented nanodomains is likely caused by a misalignment of the film positioned on the AFM substrate). Under the conditions employed, LC orientation, P3HT crystallization, and microphase separation were likely to be decoupled events. We observed that if a BCP film was first annealed at 220 °C to obtain a nicely phase-separated morphology (Figure 2a), the same photophysical and thermal treatment could not align the nanodomains of P3HT. The results show that the photoinduced orientation of azobenzene mesogens could also be used to align macroscopically the nanodomains of P3HT, but to a lesser degree because of lower annealing temperatures required to retain the orientation of azobenzene mesogens.

In summary, we synthesized the first diblock copolymer composed of regioregular P3HT and a SCLCP. By designing a BCP that contains an SCLCP block with a clearing temperature higher than the melting temperature of the crystalline P3HT, we found that both surface- and photoinduced orientation of azobenzene mesogens in the PAzoMA major phase could be used to impose a macroscopic orientation of the stripelike nanodomains of P3HT in the same direction as the mesogens. In view of the great ease and variety of field-induced controllable LC orientation, this study has demonstrated how macroscopically ordered microstructures or morphologies of BCPs based on π-conjugated polymers can be formed and manipulated. The use of this approach to induce oriented nanodomains of both donors and acceptors in a BCP, which is a requirement for photovoltaic applications, however, remains a challenge. One possible strategy is to develop donor–acceptor diblock copolymers of which one block itself is an LCP. As an alternative, ABC triblock copolymers could be designed, where A and B are donor and acceptor blocks and C is an SCLCP. If field-induced LC orientation aligns microphase-separated domains of A and B, it will be necessary to find a way to selectively degrade the SCLCP block while retaining the continuous phases of donor and acceptor blocks. Work aimed at addressing these issues is currently underway.

Received: July 20, 2010
Published online: October 19, 2010

Keywords: azobenzene · block copolymers · conducting materials · liquid crystals · surface chemistry

[1] a) R. A. Segalman, B. McCulloch, S. Kirmayer, J. J. Urban, *Macromolecules* **2009**, *42*, 9205–9216; b) U. Scherf, A. Gutacker, N. Koenen, *Acc. Chem. Res.* **2008**, *41*, 1086–1097.

[2] P. T. Wu, G. Ren, C. Li, R. Mezzenga, S. A. Jenekhe, *Macromolecules* **2009**, *42*, 2317 – 2320.
[3] B. W. Boudouris, C. D. Frisbie, M. A. Hillmyer, *Macromolecules* **2010**, *43*, 3566 – 3569.
[4] I. Botiz, S. B. Darling, *Macromolecules* **2009**, *42*, 8211 – 8217.
[5] Y. Zhang, K. Tajima, K. Hashimoto, *Macromolecules* **2009**, *42*, 7008 – 7015.
[6] C. P. Radano, O. A. Scherman, N. Stigelin-Stutzmann, C. Müller, D. W. Breiby, P. Smith, R. A. J. Janssen, E. W. Meijer, *J. Am. Chem. Soc.* **2005**, *127*, 12502 – 12503.
[7] C. R. Craley, R. Zhang, T. Kowalewski, R. D. McCullough, M. C. Stefan, *Macromol. Rapid Commun.* **2009**, *30*, 11 – 16.
[8] H. Yu, J. Li, T. Ikeda, T. Iyoda, *Adv. Mater.* **2006**, *18*, 2213 – 2215.
[9] H. Yu, T. Iyoda, T. Ikeda, *J. Am. Chem. Soc.* **2006**, *128*, 11010 – 11011.
[10] Y. Morikawa, S. Nagano, K. Watanabe, K. Kamata, T. Iyoda, T. Seki, *Adv. Mater.* **2006**, *18*, 883 – 886.
[11] Y. Morikawa, T. Kondo, S. Nagano, T. Seki, *Chem. Mater.* **2007**, *19*, 1540 – 1542.
[12] a) M. Han, K. Ichimura, *Macromolecules* **2001**, *34*, 90 – 98; b) A. Natansohn, P. Rochon, *Chem. Rev.* **2002**, *102*, 4139; c) Y. Wu, Q. Zhang, A. Kanazawa, T. Shiono, T. Ikeda, Y. Nagase, *Macromolecules* **1999**, *32*, 3951 – 3956; d) L. Cui, Y. Zhao, A. Yavrian, T. Galstian, *Macromolecules* **2003**, *36*, 8246 – 8252.
[13] Y. Zhao, X. Tong, Y. Zhao, *Macromol. Rapid Commun.* **2010**, *31*, 986 – 990.
[14] M. Jeffries-EL, G. Sauvé, R. D. McCullough, *Macromolecules* **2005**, *38*, 10346 – 10352.
[15] A. Ohira, T. M. Swager, *Macromolecules* **2007**, *40*, 19 – 25.

Angewandte Chemie
Eine Zeitschrift der Gesellschaft Deutscher Chemiker

Supporting Information

69451 Weinheim, Germany

Block Copolymers Comprising π-Conjugated and Liquid Crystalline Subunits: Induction of Macroscopic Nanodomain Orientation**

*Dehui Han, Xia Tong, Yi Zhao, and Yue Zhao**

anie_201004445_sm_miscellaneous_information.pdf

1. Block Copolymer Synthesis

Scheme 1 shows the synthetic route to the BCP by using ATRP. The P3HT macroinitiator and the azobenzene monomer, 4-[4-(6-methacryloyoxyhexyloxy)benzoate]-4'-hexyloxyazobenzene (AzoMA), were synthesized using methods reported in the literature,[1,2] and details will not be repeated here.

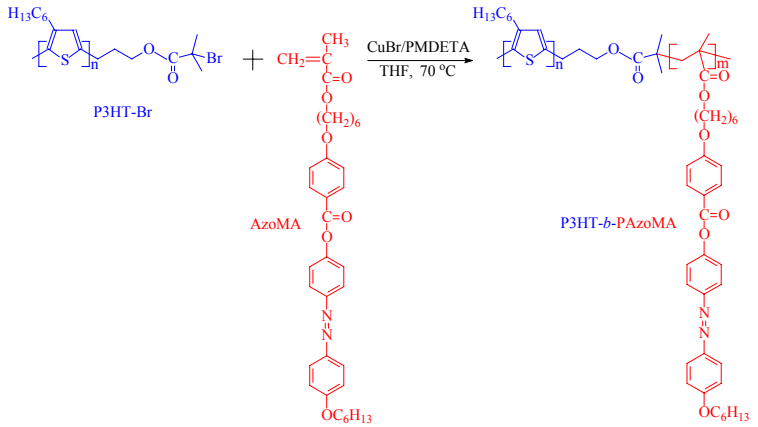

Scheme S1. Synthetic route to P3HT-*b*-PAzoMA block copolymer.

Materials. Tetrahydrofuran (THF, 99%) was refluxed with sodium and a small amount of benzophenone and distilled. Triethylamine (TEA) (Aldrich, ≥99) was refluxed with *p*-toluenesulfonyl chloride (Fluka, ≥99%) and distilled prior to use. Copper(I) bromide (CuBr, 99.999%), α-bromoisobutyryl bromide (98%), *N,N,N',N'',N''*-pentamethyldiethylenetriamine (PMDETA, 99%), *N*-bromosuccinimide (99%), [1,3 bis(diphenylphosphino)propane], dichloronickel(II) (Ni(dppp)Cl_2), 3-hexylthiophene (≥99%), allylmagnesium bromide solution (1 *M*, in diethyl ether) and 9-borabicyclo[3.3.1]nonane solution (0.5 M in THF) (9-BBN) were purchased from Aldrich and used directly.

Preparation of P3HT-*b*-PAzoMA. Several samples of BCPs were prepared. As example, what follows are the synthetic details for $P3HT_{43}$-*b*-$PAzoMA_{120}$. $P3HT_{43}$-Br (0.2 g, 0.02 mmol), CuBr (2.9 mg, 0.02 mmol), AzoMA (0.5 g, 0.85 mmol), PMDETA (3.5 mg, 0.02 mmol) and 1.5 mL THF was added into a 10-mL flask. The reaction mixture was degassed by three-pump-thaw cycles, back-filled with argon and placed in an oil bath thermostated at 70 °C for 5 h. The mixture was then diluted with THF and passed through a column of neutral alumina to remove the metal salt. After precipitation of THF solution in diethyl ether twice, the purple polymer was collected by filtration and then dried under vacuum overnight (0.53 g, 76%).

Fractionation of BCP samples. A small amount of un-reacted P3HT remained after the BCP synthesis using ATRP. They were easily removed by fractionation precipitation. As example, 0.36 g of BCP was dissolved into 100 mL of THF, then 80 mL of hexanes was added dropwise to the solution until it turned cloudy and some precipitant came out. Following a centrifuge, the precipitated BCP was collected and dried in vacuum oven at room temperature for 24 h, yielding 0.20 g of P3HT-*b*-PAzoMA free of P3HT homopolymers (Fig.1a).

2. Characterizations

^{1}H NMR spectra were recorded on a Bruker 600 MHz spectrometer using deuterated chloroform as solvent and tetramethylsilane as internal standard. The spectra were used to determine the number-average molecular weights (M_n) of P3HT macroinitiators. A Waters size exclusion chromatograph (SEC) instrument, equipped with a Waters 410 differential refractometer detector and a Waters 996 photodiode

array detector, was also utilized to measure the M_n, M_w (weight-average molecular weight) and the polydispersity index (PDI) using polystyrene (PS) standards. The SEC measurements were conduced at 35 ^oC using one column (Waters Styragel HR4E, 7.8 mm × 300 mm, 5 μm beads) and THF eluent (flow rate: 1.0 mL min^{-1}). A TA Q200 differential scanning calorimeter (DSC) was used to investigate the phase transition behaviours, using indium as the calibration standard and a heating or cooling rate of 10 ^oC min^{-1}. Glass transition temperature (T_g) was measured as the midpoint of the change in heat capacity, while mesophase transition temperatures were taken as the maximum of the respective endothermic peak (on heating) or exothermic peak (on cooling). UV-vis absorption spectra were obtained with a Cary 50 spectrophotometer (Varian), while fluorescence emission spectra were recorded using an Eclipse spectrometer of fluorescence (Varian). Polarizing optical microscopic (POM) observations were carried on a Leitz DMR-P microscope equipped with an Instec hot stage. X-ray diffraction (XRD) measurements were performed using a Siemens diffractometer, with graphite monochromatized copper radiation (K□ □1.5418 Å). To record the diffraction patterns of a sample, it was inserted in a thin-walled (0.01 mm) glass capillary tube (1.0 mm diameter) and the sample temperature was controlled with a custom modified HCS400 Instec hot stage equipped with a STC200D controller. Tapping-mode atomic force microscopy (AFM, Nanoscope IV) was utilized to examine the phase-separated morphology of thin films cast from a chlorobenzene solution on a quartz or rubbed glass plate. For photoinduced orientation, UV (λ = 360 nm, 10 mW/cm^2) and visible light (λ = 440 nm, 1.4 mW/cm^2) were produced by a spot-curing system (Novacure 2100) combined with interference filters (10 nm bandwidth, Oriel). Polarized Raman spectra were recorded on a Jobin Yvon HR800 microspectrophotometer using the 633 nm excitation from a He-Ne laser, changing the polarizations of the laser and the analyser.

3. ^{1}H NMR Spectra

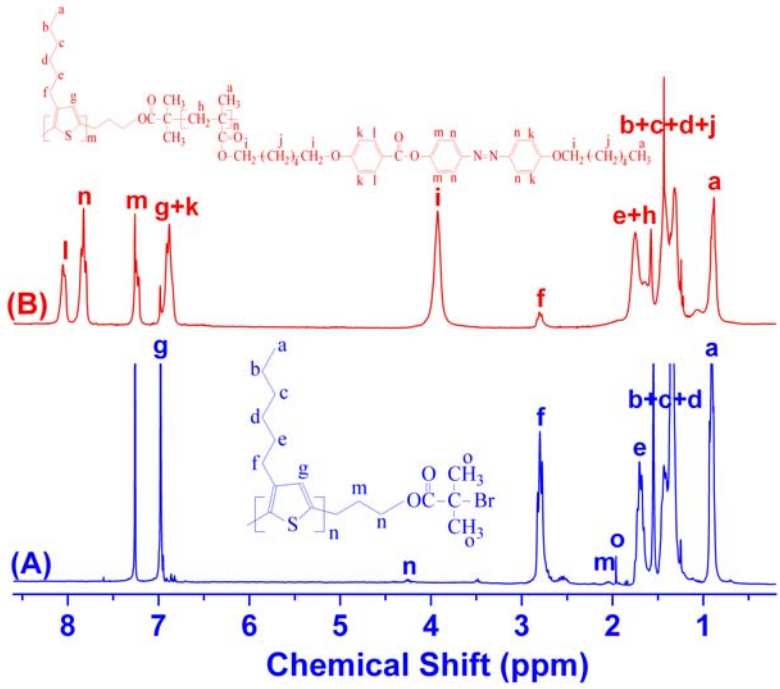

Figure S1 Examples of ^{1}H NMR spectra with (A) $P3HT_{43}$-Br and (B) $P3HT_{43}$-*b*-$PAzoMA_{120}$. The spectrum of P3HT-Br was used to determine its number-average molecular weight by comparing the integral of peak f at δ=2.80-2.90 ppm and that of peak n at δ=4.26 ppm, yielding M_n=7330 g/mol and

degree of polymerization DP=43 for P3HT. The spectrum of the copolymer was then used to determine its composition by comparing the integrals of peak l at δ=8.12 ppm and that of peak f at δ=2.80-2.90 ppm, leading to DP=120 for the block of PAzoMA.

4. DSC Curves

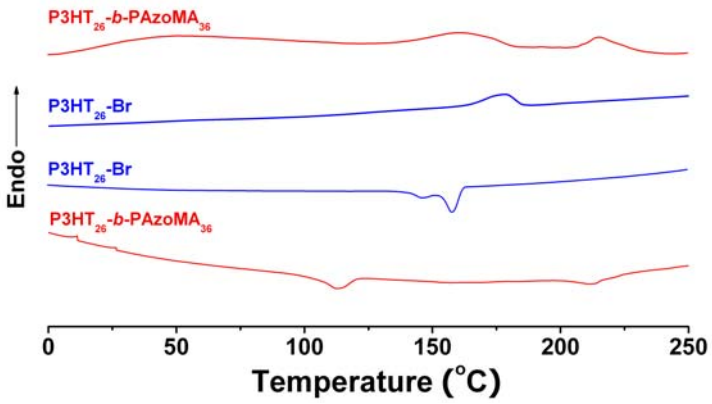

Figure S2 DSC heating and cooling curves of $P3HT_{26}$-Br and $P3HT_{26}$-*b*-$PAzoMA_{36}$. As compared to the curves for $P3HT_{43}$-Br and $P3HT_{43}$-*b*-$PAzoMA_{120}$ (Fig.1b), it is clear that the phase transition temperatures depend on the molecular weight of the P3HT macroinitiator and the BCP composition.

5. Polarizing Optical Micrographs

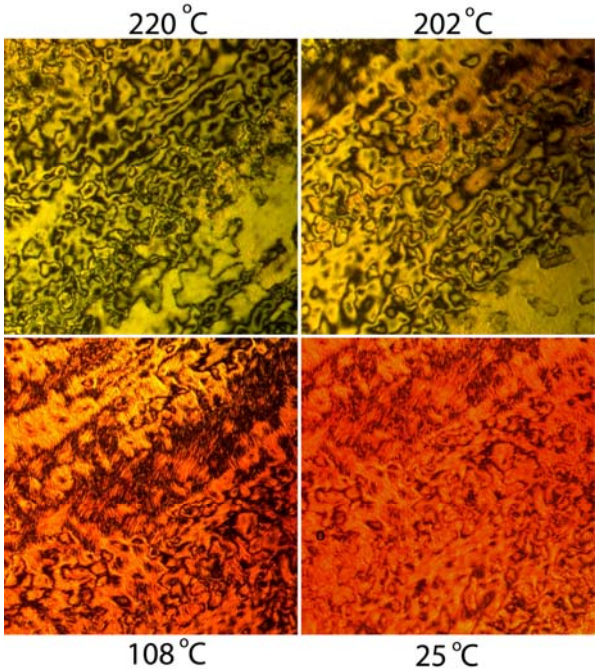

Figure S3 Polarizing optical microscope (POM) images for $P3HT_{43}$-*b*-$PAzoMA_{120}$ taken at different temperatures upon cooling from 265 °C (isotropic phase) (picture size: 296 μm× 296 μm). At 220 °C the threaded texture indicates a nematic phase of PAzoMA, though X-ray diffraction reveals the existence of

a smectic ordering; while at 202 ^{o}C, the change in texture (appearance of striation) indicates a more ordered smectic phase of PAzoMA, which is consistent with the X-ray diffraction results. At 108 and 25 ^{o}C, the crystallization of the P3HT gives rise to the change in the texture and apparent birefringence, and the color change is caused by the absorption of P3HT.

6. X-ray Diffraction

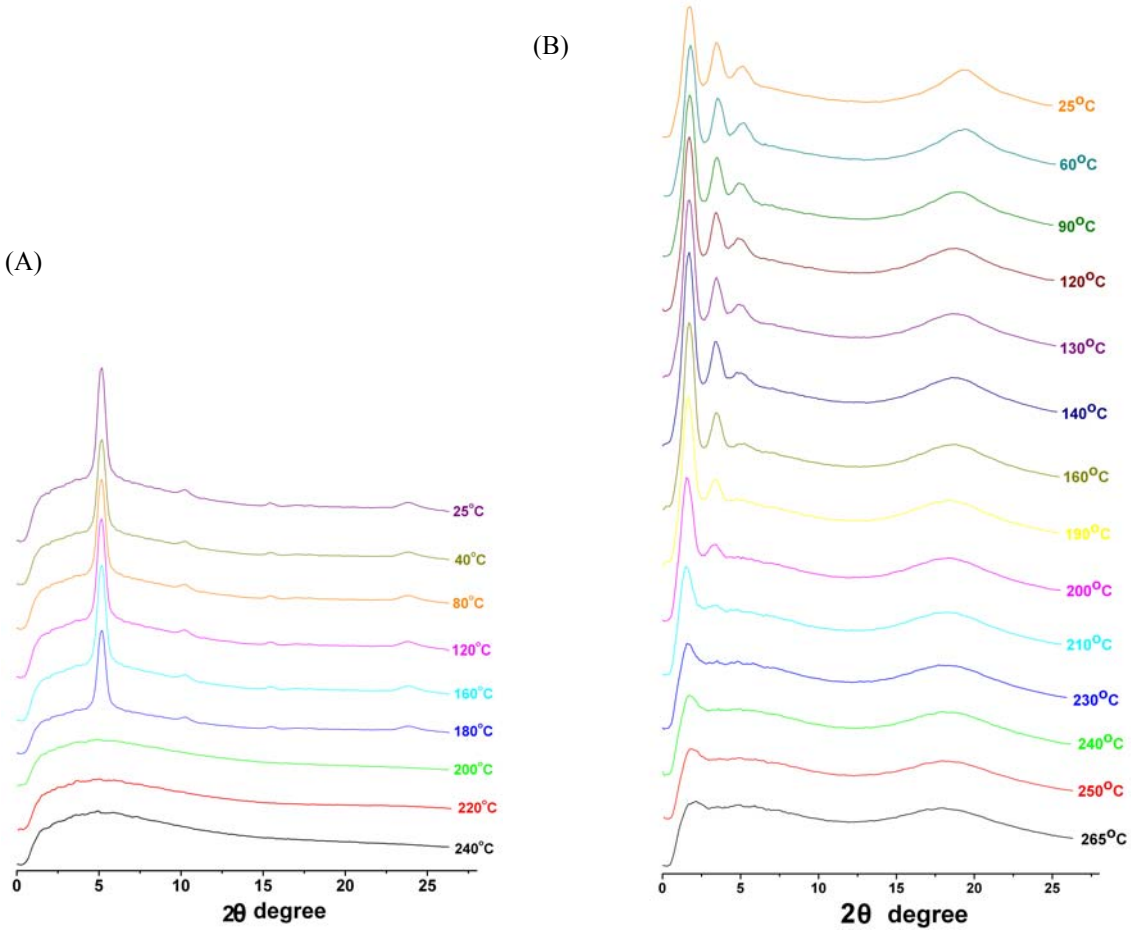

Figure S4. Variable-temperature X-ray diffraction patterns of (A) $P3HT_{43}$-Br and (B) $P3HT_{43}$-*b*-$PAzoMA_{120}$ on cooling from the isotropic state.

7. UV-vis and Fluorescence Emission Spectra

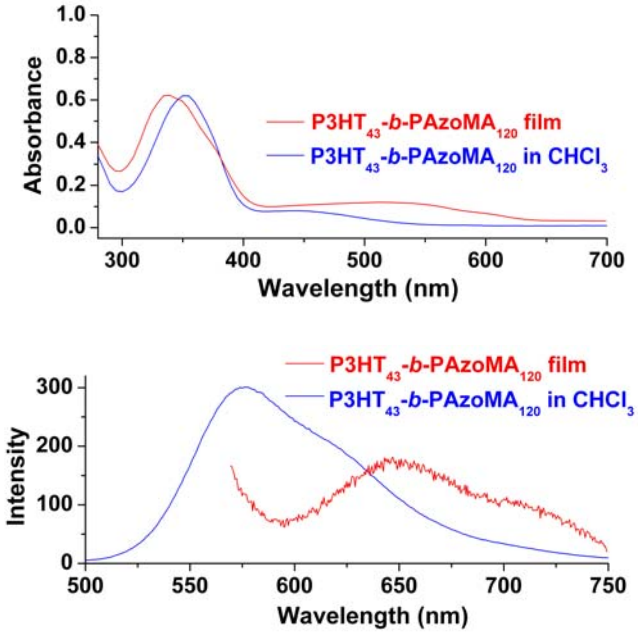

Figure S5. UV-vis (top) and fluorescence emission spectra (bottom) of $P3HT_{43}$-*b*-$PAzoMA_{120}$ in $CHCl_3$ and in the solid state (thin film). Azobenzene absorption maximum displays a blue-shift from 352 nm in solution to 336 nm in film due to an increased amount of H-aggregation of azobenzene mesogens in the solid state. By contrast, the absorption maximum of P3HT showes a red-shift from 450 nm in solution to 545 nm in the film due to packing of conjugated polymer chains in the latter. The shift of P3HT absorption maximum results in a shift of its fluorescence emission maximum from 575 nm (λ_{ex}=480 nm) in solution to 650 nm for the film.(λ_{ex}=550 nm).

8. Polarized Raman Spectroscopic Measurements

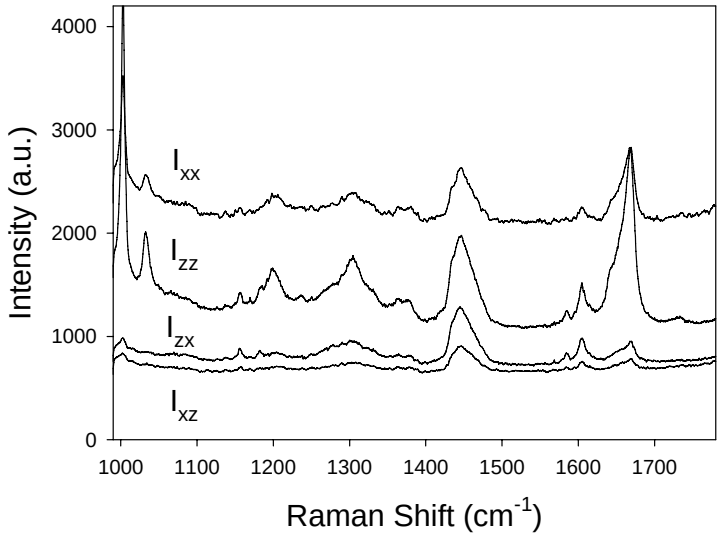

Figure S6. Polarized micro-Raman spectra recorded on the surface-oriented $P3HT_{43}$-*b*-$PAzoMA_{120}$ film used for the AFM observation (Fig.2b) The polarization of the excitation laser beam, propagating along

the *y*-axis of the coordinate system, was set to be parallel and perpendicular, respectively, to the rubbing direction, i. e., along the *z* and *x* axis. For each laser polarization, emissions were recorded with the polarization of the analyser set to be parallel and perpendicular to the laser polarization. This yields Raman spectra of I_{zz}, I_{zx}, I_{xx} and I_{xz} (the 1st letter in the subscript indicates the polarization of the laser beam and the 2nd letter the polarization of the analyser). Similar to polarized UV-vis spectra (Fig.2b), the strong dichroism indicates orientation of mesogens along the rubbing direction. Unfortunately, peaks assigned to stretching modes of thiophene rings (around 1460 cm^{-1}) [3] are overlapped by peaks of azobenzene mesogens, making it impossible to assess orientation of P3HT chains confined in the nanodomains.

9. AFM

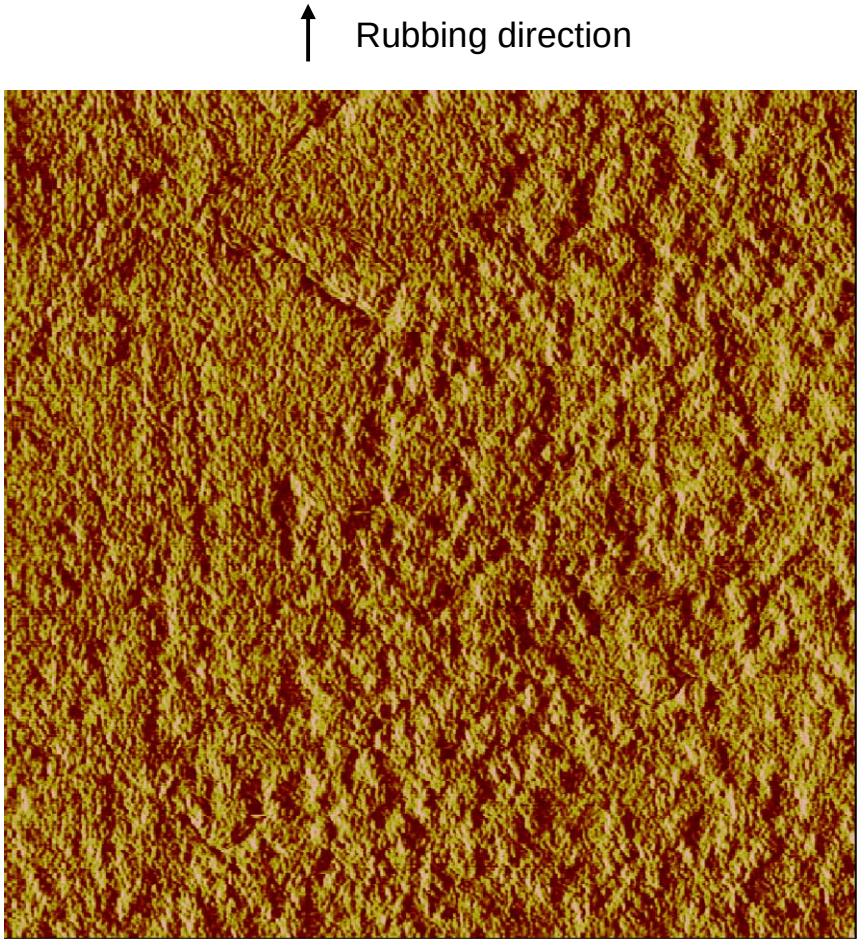

Figure S7. AFM phase image of a surface-oriented $P3HT_{43}$-*b*-$PAzoMA_{120}$ film over an area of 5 μm × 5 μm. Surface roughnesses of the films is below 8 nm.

References

[1] M. Jeffries-EL, G. Sauvé, R.D. McCullough, Macromolecules 2005, 38, 10346-10352.
[2] Y. Zhao. X. Tong. Y. Zhao, Macromol. Rapid Commun. 2010, 31, 986-990.
[3] M.C. Gather, D.C. Bradley, Adv. Funct. Mater. 2007, 17, 479-485.